

Direct Evidence for Shallow Acceptor States with Nonspherical Symmetry in GaAs

G. Mahieu,¹ B. Grandidier,¹ D. Deresmes,¹ J. P. Nys,¹ D. Stiévenard,¹ and Ph. Ebert²

¹Institut d'Electronique, de Microélectronique et de Nanotechnologie, IEMN, (CNRS, UMR 8520), Département ISEN, 41 bd Vauban, 59046 Lille Cedex, France

²Institut für Festkörperforschung, Forschungszentrum Jülich GmbH, 52425 Jülich, Germany

(Received 22 June 2004; published 20 January 2005)

We investigate the energy and symmetry of Zn and Be dopant-induced acceptor states in GaAs using cross-sectional scanning tunnelling microscopy (STM) and spectroscopy at low temperatures. The ground and first excited states are found to have a nonspherical symmetry. In particular, the first excited acceptor state has a T_d symmetry. Its major contribution to the STM empty-state images allows us to explain the puzzling triangular shaped contrast observed in the empty-state STM images of acceptor impurities in III-V semiconductors.

DOI: 10.1103/PhysRevLett.94.026407

PACS numbers: 71.55.Eq, 68.37.Ef

Dopant atoms govern many of the technologically most interesting properties of semiconductors, by introducing shallow acceptor or donor states. These are thermally ionized and thereby provide free charge carriers. It is generally assumed that each free carrier interacts with its charged dopant atom in analogy to the hydrogen atom model. In this textbook picture, the local potential associated with the dopant atom has a *spherical symmetry*, which is consistent with the screened Coulomb potential surrounding every electrically active dopant [1]. As a consequence the wave functions of acceptor or donor atoms can be described by hydrogenic wave functions [2].

However, diamond and zinc blend semiconductors have a cubic symmetry. The formation of acceptor states from the nonspherical valence band states of the cubic host lattice should in principle affect the wave functions of the acceptor states and therefore the interaction of dopants with free carriers. Such interaction is of prime importance for the down scaling of semiconductor devices, where the conductance relies on individual dopant atoms and the ferromagnetism coupling depends on the strength of the impurity-impurity interaction mediated by free carriers.

Although the cubic symmetry prevailed to explain additional lines observed in the excitation spectra of acceptors [3], and the spatial shape of deep Mn acceptor ground state in GaAs mapped by STM [4], the empty-state STM images of shallow acceptors [5,6], which differs readily from those observed for Mn acceptors, appear neither compatible with a simple spherical description, nor with a cubic crystal symmetry. Therefore, we investigated here in detail the electronic properties of shallow acceptor states induced by *p*-type dopant atoms in GaAs.

Combining the high spatial resolution and high electronic sensitivity of the STM at 5 K, we identify the energy and symmetry of the ground as well as the first two excited acceptor states. In particular, we show that the first excited state exhibits a T_d symmetry with the density of states concentrated in four tetrahedrons extending along the four equivalent $\langle 111 \rangle$ directions, due to the anisotropy of the valence band states. The intersection of the cleavage

surface with the tetrahedrons of the first excited acceptor state leads to the imaging of the triangular contrasts in STM images.

For our experiments we cleaved Zn and Be-doped GaAs crystals along (011) and (01 $\bar{1}$) surfaces in ultrahigh vacuum ($<1 \times 10^{-8}$ Pa). Consistent with the bulk concentration of the dopants we observed features as shown in Fig. 1 on the freshly cleaved surfaces. These features arise from bulk dopant atoms in the first few subsurface layers exposed by cleavage. At negative voltages, the dopant atoms give rise to a white elevation [Fig. 1(a)] superimposed on the atomic corrugation showing the occupied arsenic (As) derived dangling bond states (called A_5). This elevation in constant-current STM images has been interpreted as the image of the local screened Coulomb potential-induced band bending surrounding the charged dopant.

At small positive voltages [Fig. 1(b)], the contrast of the dopant changes to a triangular shape, superimposed on the empty gallium (Ga) derived dangling bonds (called C_3). By comparing the symmetry and the contrast intensity of the acceptor relative to the background As sublattice, the projected position of the dopant atoms is localized at the

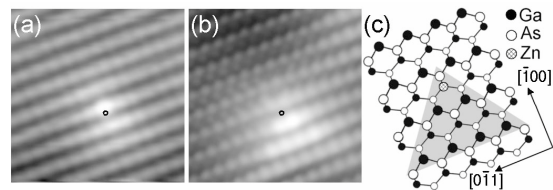


FIG. 1. STM images of a Zn dopant atom localized in a *p*-type GaAs(110) cleavage surface (carrier concentration $2 \times 10^{19} \text{ cm}^{-3}$) acquired at 5 K with sample voltages V_s of (a) -1.8 V and (b) $+1.7$ V. From the analysis of the contrast symmetry and intensity (Ref. [8]), the Zn dopant, whose projected position is indicated by a black circle, is found to be located in the second layer. (c) Schematic view of the GaAs (110) surface showing the first (larger circles) and second layer Ga and As atoms and a shaded area corresponding to the triangular contrast visible in (b).

apex of the triangular contrast, while the main part of the triangle extends along a $\langle 100 \rangle$ direction away from the projected dopant position [Fig. 1(c)]. These observations are corroborated by a number of previous results of Zn and Cd dopants in GaAs as well as Zn and Sn dopants in InP [5–7].

Although the orientation of the triangular contrast is always the same for all dopant atoms in one sample, there are crucial differences if we compare (011) and (01 $\bar{1}$) cleavage surfaces. These two surfaces represent perpendicular cross-sections through the crystal. Figs. 2(a) and 2(b) show that the triangular contrasts have opposite orientations on the (011) compared to the (01 $\bar{1}$) surface with respect to the [100] direction. Since the orientation of the zig-zag rows is inverted for both surfaces, this is consistent with the observation of oppositely oriented triangles.

Furthermore, knowing the depth of the dopant atom from symmetry and apparent height changes of the triangular shape [8], we see that its lateral size is increasing with increasing depth of the dopant below the surface [Fig. 2(c)]. This indicates that this feature is indeed bulk related and not an artifact of the surface. Its shape can be deduced from the orientation of the edges of the triangular contrast. The two side edges run along $\langle 211 \rangle$ directions, whereas the base is oriented along a $\langle 011 \rangle$ direction. All

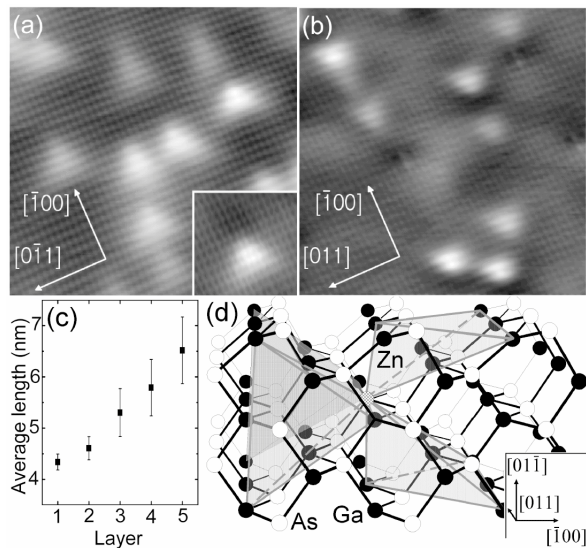


FIG. 2. Orientations of the triangular contrast for the two perpendicular cleavage planes of a [100]-oriented Zn-doped *p*-type GaAs wafer (doping concentration $2.0 \times 10^{19} \text{ cm}^{-3}$): STM images of (a) (011) and (b) (01 $\bar{1}$) surfaces acquired at 77 K, $V_s = +1.70 \text{ V}$. Inset: Be-doped GaAs(011) surface with doping concentration $2.0 \times 10^{18} \text{ cm}^{-3}$ observed at 5 K, $V_s = +1.65 \text{ V}$. (c) Size of the triangular contrasts measured along their $\langle 112 \rangle$ edges as a function of the depth of the dopant atom (surface layer equals layer 1). (d) Schematic view of the cubic T_d geometrical configuration deduced from the observations (a) to (c). Four tetrahedronlike features extend along the four equivalent $\langle 111 \rangle$ directions.

three are intersection lines of the surface with three $\{111\}$ planes. Furthermore the slope of the increase in size ($0.5 \pm 0.15 \text{ nm/layer}$ along a $\langle 211 \rangle$ direction) is consistent with a tetrahedrally shaped bulk feature, whose sides are delimited by $\{111\}$ planes (results in a slope of 0.35 nm/layer). The intersection of the surface plane with the tetrahedrally shaped bulk feature yields then the triangular contrasts.

The above observations are leading us to a geometry of the dopant-induced feature dominated by four tetrahedrally shaped features, extending away from the dopant in all four equivalent $\langle 111 \rangle$ directions [Fig. 2(d)]. The tips of the tetrahedrons meet at the dopant's position. This corresponds to a cubic T_d symmetry. If we now look at one of the two possible cleavage surfaces we can only see an intersection plane with one of the four tetrahedrons giving a triangular contrast. Since we observe it only for dopants in the first six layers, each tetrahedron extends about 1.5 nm along a $\langle 111 \rangle$ direction. A detailed analysis of the intensity of the triangular contrast along the [100] direction furthermore suggests a progressive weakening of the density of states (DOS) within the tetrahedron reaching the sensitivity limit of the STM at a distance of about 1.5 nm . Note that the contrasts observed in the STM images must be entirely electronic, because strain would yield significant differences between Be, Zn (compare inset of Fig. 2(a) with Fig. 2(a) and 2(b)), and Cd dopant atoms [6], in contrast to the observations.

At this stage we turn to the electronic origin of the triangular contrast. This contrast is seen in a narrow range of positive voltages, generally from $+1.6$ to $+1.8 \text{ V}$ [Fig. 3(a)]. At such voltages the tip of the STM induces an upward band bending on *p*-type surfaces, leading to an accumulation zone below the tip [9]. This enables the electrons from the tip to tunnel into emptied valence band states. Indeed, when imaging the filled states at the top of the valence band with small negative sample voltages, the dopants appear as triangular contrasts too [Fig. 3(b) and 3(c)]. Therefore, the triangular contrast is caused by a modification of the DOS at or close to the top of the valence band.

To further explore the variation of the DOS in the valence band arising from the presence of a dopant atom, we performed spatially resolved spectroscopic measurements of the tunnelling current and the conductivity, using a similar method as the one used in Ref. [8]. The measure-



FIG. 3. STM images of two Zn dopant atoms in the GaAs (011) surface acquired at 5 K with sample voltages of (a) $+1.8 \text{ V}$, (b) -0.1 V , and (c) -0.2 V .

ment of the normalized conductivity $(dI/dV)/(I/V)$ obtained outside of the triangular contrast of a fourth layer dopant atom [spectrum B in Fig. 4(a1)] yields clearly the valence (at negative voltages) and the conduction band components (above about +1.5 eV), separated by a band gap region about 1.5 eV wide, consistent with the GaAs band gap at 5 K. The Fermi level E_F (at 0 V) is positioned above the top of the valence band, in agreement with a p -type sample at 5 K.

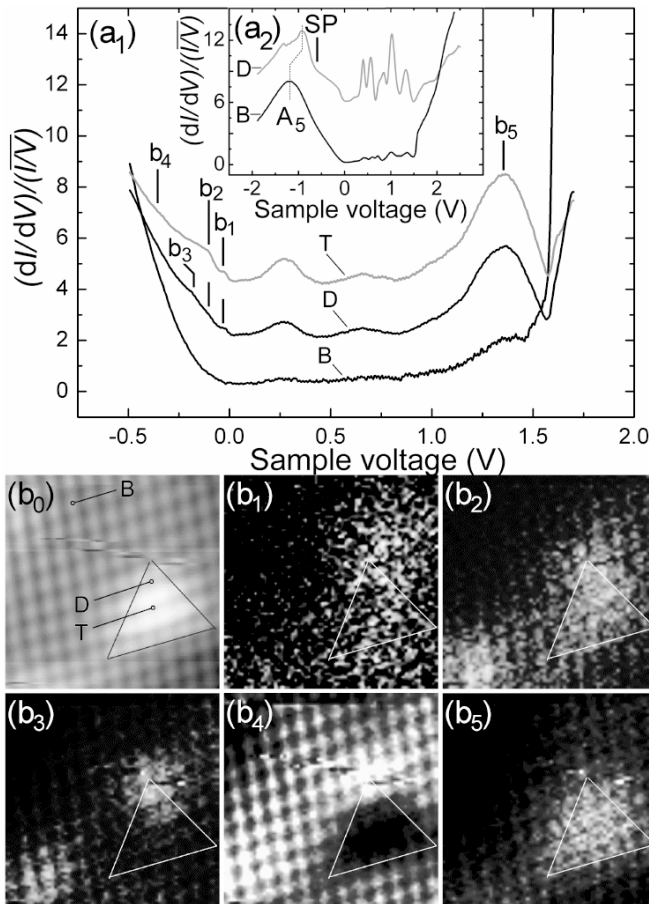


FIG. 4. Spatially resolved tunneling spectroscopic measurements obtained at 5 K on a Zn-doped p -type GaAs (011) surface. (a1) Tunneling spectra acquired at *fixed* tip-to-sample distance at the location of the dopant atom (D) belonging to the 4th layer, in the center of the triangular contrast (T), and on the bare surface (B). Particular spectral features, labeled b_1 to b_5 , are positioned at energies of -0.02 eV, -0.10 eV, -0.15 eV, -0.35 eV, $+1.33$ eV, respectively. (a2) Tunneling spectra acquired at *variable* tip-to-sample distance in the center of the triangular contrast (T) and on the bare surface (B). Onset energy for the split-off energy is marked by line SP (see text). In each frame the spectra have been shifted for clarity. (b) dI/dV conductivity maps obtained in the area shown in the topographic image b_0 for the energies corresponding, respectively, to the lines b_1 to b_5 . The triangle should guide the eye to compare the pictures. At the bottom left of the images, a dopant located in the sixth layer is also present.

In contrast to the monotonous exponential increase of the signal in the valence band far away from the dopant (spectrum B), the variations of the signal are quite different at the location of the dopant [spectrum D in Fig. 4(a1)] and in the center of the triangular contrast [spectrum T in Fig. 4(a1)]. Distinct features are found, which are induced by the dopant as outlined below: (i) a peak (labeled b_1) is found at $E_F - 0.02 \pm 0.01$ eV at the location of the dopant and in the triangular contrast, (ii) a step (labeled b_2) is observed at $E_F - 0.10 \pm 0.01$ eV in the triangular contrast, (iii) a less pronounced step (labeled b_3) is seen at $E_F - 0.15 \pm 0.01$ eV at the location of the dopant, (iv) the signal increases more slowly in the triangular contrast than in the bare surface around the energy marked b_4 . This reduced DOS extends up to $E_F - 0.66 \pm 0.01$ eV (as visible and marked by SP in the enlarged voltage scan shown in Fig. 4(a2)).

In addition, within the band gap region several peaks exist, whose number, position, and intensity are very dependent on the tip and tunnelling conditions. This becomes obvious when comparing Fig. 4(a1) (fixed tip-to-sample separation) with Fig. 4(a2), where a variable tip-sample distance was used. Such peaks were observed before at 5 K in the band gap of semiconductors [9,10]. These peaks are associated with the formation of a confining three-dimensional band bending region in the sample below the tip.

In order to discuss the origin of the three lines observed close to the top of the valence band, we evaluate the tip-induced band bending in the semiconductor region solving the one-dimensional Poisson's equation as described in Ref. [11]. Taking as parameters a tip-sample distance of 0.9 nm, a tip work function of 4.5 eV, an electron affinity and a band gap of 4.07 eV and 1.52 eV for GaAs, respectively, and a doping density of $2 \times 10^{19} \text{ cm}^{-3}$, we find the top of the valence band to be positioned 0.16 eV below the Fermi level at 0 V. Based on the position of the valence band edge, we find that features b_1 , b_2 , and b_3 are 0.14 ± 0.01 eV, 0.06 ± 0.01 eV, 0.01 ± 0.01 eV above the valence band edge, respectively.

These binding energies are expected to deviate from the bulk binding energy of 31.3 meV [12]: (i) Since the dopant atom is close to the surface, the dielectric constant is the average of GaAs and vacuum, which leads to an increase of the binding energy by almost a factor of $2^2 = 4$. (ii) In addition, the tip induces a localized depletion zone, which forms a confining potential approximately triangularly shaped and about three to 5 nm wide in the direction perpendicular to the surface. Along the surface, due to the relatively large radius of curvature of the tip (compared to the tip-sample separation), the confining potential is much more extended, such that a one-dimensional approximation of the confining potential is sufficient. A dopant 0.6 nm below the surface is located close to the edge of such a confining potential. In this case one expects a further

shift of the bulk binding energy by a factor of about 1.2 to 1.4 [13]. Thus one would expect for the ground state a binding energy between 130 and 150 meV in the tunneling spectra, consistent with the observed binding energy of 140 meV for the peak b_1 . Therefore we attribute peak b_1 to the acceptor ground state. Similarly, the binding energy of the excited states should also be increased. We identify thus lines b_2 and b_3 to arise from the first two excited states.

In order to investigate the symmetry of the individual acceptor states, dI/dV maps of a dopant atom in the fourth layer were recorded. The conductivity map taken at the energy of line b_1 [Fig. 4(b1)] shows that the intensity distribution, which corresponds to the probability density of the acceptor ground state, has clearly not a spherical symmetry. The distribution extends more along the $\langle 100 \rangle$ direction in agreement with the wave function obtained for Mn acceptor in GaAs. Similarly, the conductivity map acquired at the energy of line b_2 indicates that the intensity distribution is not centered on the dopant atom, but spreads out in the region of the triangular contrast [Fig. 4(b2)], consistent with the topographic images at very small negative voltages shown in Fig. 3. Probing the third acceptor states just above the edge of the valence band (at a voltage of -0.15 V, marked by b_3), we observe that the intensity distribution of the DOS has a circular symmetry centered at the location of the dopant atom [Fig. 4(b3)].

From these observations, we can deduce the contribution of the different acceptor states to the tip-induced states observed in the band gap region of Fig. 4(a1) and 4(a2). Figure 4(b5) shows that the density of states at the energy of peak b_5 has an intensity distribution, which is closest to the distribution obtained for the first excited state. As a result, peak b_5 results from the resonance of the first excited state with tip-induced states. The high intensity of this peak dominates the tunnel current even at voltages up to about $+1.8$ V and thus gives rise to the triangular feature observed in the topographic images. From the topographic image of Fig. 3(a) and 3(b) and the observation of Fig. 4(b2) and 4(b5), we conclude that the first excited state has a T_d symmetry. While its contribution dominates the tunnelling current when the lowest conduction band states are probed, this result differs from the empty-state STM image of Mn acceptor [4]. In this case, only the ground state is involved in the tunnelling current due to the low doping level of the sample.

To discuss the origin of this symmetry, we note that in the valence band [Fig. 4(b4)] a strong decrease of the DOS appears in the region of the triangular contrast. The spectroscopic curves in Fig. 4(a2) show that the spatially limited decrease of the DOS ends at -0.66 V (line SP). Taking into account the surface band bending of -0.32 eV, the DOS in the valence band is thus reduced up to $E_F - 0.34 \pm 0.01$ eV. This value agrees well with the energy of the split-off band in GaAs [14], indicating that

primarily the states of the heavy hole (HH) and light hole bands are involved in the formation of the acceptor states.

If an acceptor impurity is incorporated in GaAs, the associated potential repels the states of the valence band, which in turn are shifted higher in energy and form the acceptor states. The ground state likely originates from the highest states at the top of the valence band near the Γ point. The first excited state originates from states slightly deeper in the valence band dominated by the HH band. Under these conditions the available states are primarily from the HH band at nonzero k vectors, where a strong directional dependence of the effective mass occurs [3,15,16]. The largest mass (smallest curvature) is along the $\langle 111 \rangle$ direction, suggesting that the DOS along this direction and its equivalents would be favored. This is consistent with the observed T_d symmetry of the first excited state.

In conclusion, we identified the energy and symmetry of the dopant-induced ground and excited acceptor states in GaAs using low-temperature scanning tunneling microscopy and spectroscopy. The results indicate that nonspherical acceptor states should exist in most cubic semiconductors, due to presence of anisotropic valence bands.

This work was supported by the European Community's Human Potential Programme under contract no. HPRN-CT-2001-00320, NANOSPECTRA and partially by the Deutsche Forschungsgemeinschaft under Grant No. Eb197/2-1.

-
- [1] R. B. Dingle, *Philos. Mag.* **46**, 831 (1955).
 - [2] E. F. Schubert, *Doping in III-V Semiconductors* (Cambridge University Press, Cambridge, 1993).
 - [3] A. Baldereschi and N. O. Lipari, *Phys. Rev. B* **9**, 1525 (1974).
 - [4] A. M. Yakunin *et al.*, *Phys. Rev. Lett.* **92**, 216806 (2004).
 - [5] J. F. Zheng, M. Salmeron, and E. R. Weber, *Appl. Phys. Lett.* **64**, 1836 (1994).
 - [6] R. de Kort *et al.*, *Phys. Rev. B* **63**, 125336 (2001).
 - [7] R. de Kort, W. Kets, and H. van Kempen, *Surf. Sci.* **482-485**, 495 (2001).
 - [8] R. M. Feenstra, J. M. Woodall, and G. D. Petit, *Phys. Rev. Lett.* **71**, 1176 (1993).
 - [9] R. M. Feenstra *et al.*, *Phys. Rev. B* **66**, 165204 (2002).
 - [10] L. Perdigo *et al.*, *Phys. Rev. Lett.* **92**, 216101 (2004).
 - [11] R. M. Feenstra, J. A. Stroscio, *J. Vac. Sci. Technol. B* **5**, 923 (1987); N. Jäger *et al.*, *Phys. Rev. B* **67**, 165327 (2003).
 - [12] V. Fiorentini, *Phys. Rev. B* **51**, 10161 (1995).
 - [13] G. Bastard, *Phys. Rev. B* **24**, 4714 (1981).
 - [14] *Semiconductors : Group IV Elements and III-V Compounds*, edited by O. Madelung (Springer Verlag, Berlin, 1991).
 - [15] J. A. Kash, *Phys. Rev. B* **47**, 1221 (1993).
 - [16] W. Hackenberg and H. P. Hughes, *Phys. Rev. B* **49**, 7990 (1994).